Article

Conditions for Minimizing the Computational Complexity of the RCWA Calculation of the Diffraction Efficiency of Sawtooth Two-Layer Double-Relief Microstructures

Grigoriy Isaevich Greisukh [*] , Artem Ivanovich Antonov , Evgeniy Grigorievich Ezhov ,
Victor Anatolyevich Danilov , Boris Alexandrovich Usievich

Article

Conditions for Minimizing the Computational Complexity of the RCWA Calculation of the Diffraction Efficiency of Sawtooth Two-Layer Double-Relief Microstructures

Grigoriy I. Greisukh [1],*, Artem I. Antonov [1], Evgeniy G. Ezhov [1], Viktor A. Danilov [2] and Boris A. Usievich [3]

[1] Physics Department of Penza State University of Architecture and Construction, G. Titova Str., 440028 Penza, Russia; phisik@pguas.ru (E.G.E.); gromlord@yandex.ru (A.I.A.)

[2] Scientific and Technological Center for Unique Instrumentation of the Russian Academy of Sciences, Butlerova Str., 117342 Moscow, Russia; viktordanilov@bk.ru

[3] Prokhorov General Physics Institute of the Russian Academy of Sciences, Vavilov Str., 119991 Moscow, Russia; borisu@kapella.gpi.ru

* Correspondence: grey@pguas.ru

Abstract: In this study novel recommendations are presented and substantiated for selecting the number of modes and optical thicknesses of flat lattice slabs that make up the microreliefs, which minimize the computational complexity of the rigorous coupled-wave analysis calculation of the diffraction efficiency (DE) of a sawtooth two-layer two-relief microstructure, while maintaining the specified reliability of the calculation results. The computational complexity can be controlled by allowing one or another level of oscillation of the DE curves depend on the angle of incidence of the radiation incident on the microstructure. In particular, the complexity of the multi-thousand DE calculations in the optimization process can be reduced by using the proposed methodology as well as increased computational complexity to certify the accuracy of the solution obtained as a result of implemented optimization.

Keywords: two-layer two-relief diffractive microstructure; diffraction efficiency; scalar and rigorous theories of diffraction; rigorous coupled-wave analysis

1. Introduction

Diffractive optical elements (DOEs) with annular microstructures similar to that of a Fresnel zone plate have attracted the attention of developers of imaging optical systems because of their unique aberration properties. In the field of chromaticism, DOEs are characterized by a negative dispersion. Moreover, in the field of monochromatic aberrations, DOEs are characterized by the automatic fulfillment of the Petzval condition and a rapid convergence of the aberration expansion for planar DOEs [1,2]. Properties of DOEs included in an optical system consisting of refractive lenses provide tangible advantages.

However, the last statement is valid only if the ratio of the radiation flux diffracted into the working order to that incident on the microstructure, i.e., the diffraction efficiency (DE) of the DOE microstructure, neither falls below a given level in the entire working spectral range nor over the entire range of angles of incidence of the radiation incident on this microstructure.

The maximum DE among the existing technologies for manufacturing ring quasi-periodic microstructures is provided by relief-phase microstructures. A single-layer microstructure (Figure 1a) can have DE = 1, but only at one specific wavelength and for one specific angle of incidence of radiation, i.e., this microstructure has energy selectivity with regards to wavelength spectrum and angle of incidence. Two-layer one- or two-relief microstructures have been successfully used to suppress the spectral energy selectivity, as shown in Figure 1b–d [3–7].

The energy angular selectivity is more pronounced for two-layer microstructures than for single-layer microstructures; moreover, its minimization is ensured by minimizing the effective depths of the reliefs h_{eff} ($h_{eff} = h$, h_1, and $h_1 + h_2$ in the schemes in Figure 1b–d, respectively). Assuming that the spectral energy selectivity is suppressed, the effective depths of the reliefs are minimized using an appropriate choice of pairs of optical materials in the microstructure arrangement.
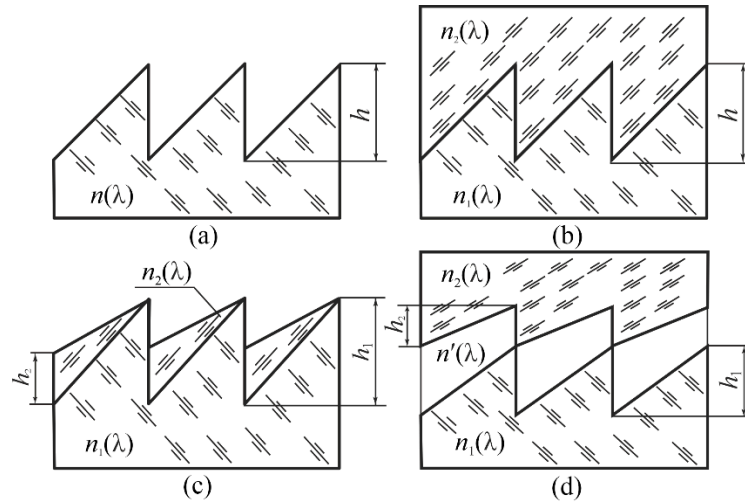

Figure 1. DOE relief-phase microstructures.

Furthermore, the catalog of optical materials from which a pair of materials can be selected for a two-layer single-relief microstructure, as shown in Figure 1b, is significantly narrow, even in the visible range. This is because a material with a high refractive index should also have a higher Abbe number, a well-known requirement for pairs of materials with two-layer single-relief microstructures [4,6]. If a certain number of such pairs, including heavy crown and light flint, are available from optical glasses, they are then completely absent from technological and commercially available optical plastics.

This limitation is eliminated owing to the two reliefs made in the two optical materials with different dispersion properties. In addition, despite the obvious appeal (in terms of angular-energy selectivity) of a microstructure with one internal relief (Figure 1c), in some cases, the choice may favor the microstructure shown in Figure 1d. This primarily applies to infrared (IR) optics that operate over a wide range of temperatures. Indeed, owing to the different thermal coefficients of linear expansion of the two layers of the microstructure, as shown in Figure 1c, ensuring mechanical strength at significantly different operating temperatures is impossible. Therefore, the most acceptable arrangement of the IR DOE microstructure currently is a two-layer microstructure with two internal sawtooth reliefs on the flat surfaces of the material substrates.

The search for optimal pairs of optical materials for the DOE microstructure is based on determining the optimal relief depths for each pair of optical materials; this requires multiple calculations of DE. As reported in [8], the results obtained based on the DEs calculated using the scalar effective area method (EAM) [9,10] are fairly reliable in the layout and calculation of microstructures intended for operation in the IR and visible range [9,10]. This applies to a greater extent to selecting the optimal pairs of optical materials, but to a lesser extent to assessing the optimal depths of the reliefs and to assessing the achievable DE.

Indeed, the degree of reliability in determining the optimal depths and achievable DE depends on the given interval of angles of incidence of radiation incident on the microstructure for the selected relative (normalized to the total depth of the reliefs) spatial period of the microstructure $P = \Lambda/(h_1 + h_2)$. Finally, these scalar results may be unreliable for microstructures with a total relief depth greater than the maximum wavelength of the working spectral range by an order of magnitude. The truly optimal relief depths of such microstructures, as well as microstructures designed for wide ranges of radiation incidence angles (±15° and more), and a reliable estimate of their DEs can only be obtained

by optimizing in the framework of rigorous diffraction theory and solving the system of Maxwell equations. In this case, a good initial approximation is obtained using the scalar EAM method.

Currently, the most common numerical methods for solving systems of Maxwell equations to calculate DE are the rigorous coupled-wave analysis (RCWA) [11] and finite-difference time-domain (FDTD) methods [9]. The insurmountable disadvantage of the latter method is that it requires considerably more computational time and computer RAM. Therefore, the RCWA method is preferred to calculate the DE of sawtooth microstructures. In particular, this method involves replacing the sawtooth relief of the diffractive microstructure with a set of flat lattice plates and applying a Fourier expansion to the periodically distributed permittivity of each plate. The accuracy of this method is determined by the optical thickness of the flat lattice slabs L that make up both microreliefs and the number of modes N_m. The computational complexity of the RCWA method depends on the aforementioned parameters.

The results of the RCWA analysis of the microstructures presented in this study are obtained using two software platforms developed with the participation of the authors of this paper, namely, PSUAC-DE [12] and MC Grating Software [13].

Considering that in the general case, the DOEs of imaging optical systems operate with unpolarized radiation, DE calculation should include calculating the efficiencies for transverse electric (TE) and transverse magnetic (TM) polarized waves; moreover, the arithmetic mean of the obtained values is considered the resulting DE. However, in the practical calculation of the DEs of all types of microstructures as shown in Figure 1, the computational complexity in the case of a TM wave is much greater, whereas the resulting efficiency values for TE and TM waves differ by no more than 2–3%. Therefore, in this study, the efficiency calculated for the TE wave is considered as the DE obtained using the RCWA method.

However, even in this case, the duration of the computational process for calculating the DE of deep relief-phase structures (two-layer microstructures with two internal reliefs) may not be acceptable for optimizing the design parameters of the microstructure. To this end, this study proposes novel recommendations for selecting the values of the main computational parameters L and N_m to ensure the minimum computational time with guaranteed reliability of the calculation results.

2. Visible spectral range

One of the most pronounced signs of the inadequacy of the values of the computational parameters L and N_m in the target problem is the oscillation of the DE curves, showcasing the dependence of DE on the incidence angle of the radiation incident on the microstructure. Evidently, oscillations prevent not only the determination of the optimal depths of the reliefs, but also a reliable assessment of the maximum permissible angle of incidence.

To clarify the causes of the oscillations and exclude the effect of Fresnel losses on the DE, antireflection coatings on the working surfaces of the microstructure are modeled into the calculation, as shown in Figure 2.
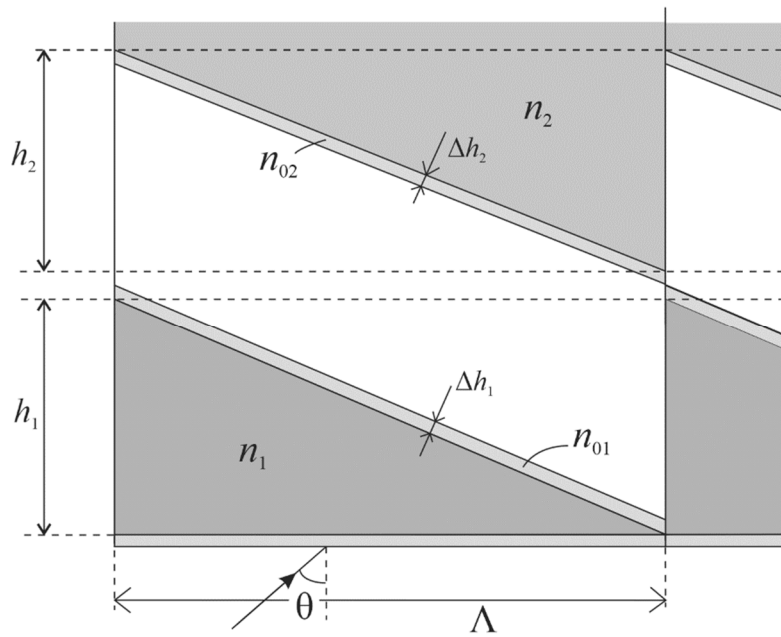
Figure 2. Two-layer two-relief microstructure with coatings deposited on the reliefs.

The space between the reliefs in the microstructure materials with refractive indices n_1 and n_2 is filled with air; moreover, the sharp peaks of the reliefs are in contact with coatings of thicknesses Δh_1 and Δh_2 and refractive indices n_{01} and n_{02}, respectively. The model coverage parameters for each wavelength are calculated using the following formulas:

$$n_{0i} = \sqrt{n_i} \; ; \quad \Delta h_i = 0.25\lambda / n_{0i} \, , \tag{1}$$

where $i = 1, 2$.

The calculations are performed for a microstructure [7] with a lower layer of E48R crown-like optical plastic ($n_d = 1.531160$; $v_d = 56.0438$) included in the ZEON catalog of the ZEMAX optical design software [14] and an upper layer of EP7000 flint-like optical plastic ($n_d = 1.651006$; $v_d = 21.4946$) manufactured by MITSUBISHI GAS CHEMICAL under the trademark Lupizeta™ EP7000 [15]. The calculations are performed in the visible spectral range from $\lambda_{min} = 0.4$ μm to $\lambda_{max} = 0.7$ μm.

In the calculations, the radiation is assumed to be incident on the microstructure from the air onto the side of the medium with refractive index n1, the angle of incidence θ is measured from the normal to the substrate, and the diffracted radiation remains in the medium with refractive index n2.

Figures 3 and 4 showcase the dependence of DE on the angle of incidence taken from the unpublished archive of the authors. The depths of the reliefs are considered optimal for each value of the relative spatial period P of the microstructure. The geometric thicknesses of the plates in the first and second reliefs are $l_{h1} = 0.11\lambda_{min}$ and $l_{h2} = 0.078\lambda_{min}$; moreover, the number of modes $N_m = 200$ ensures the absence of oscillations at $P = 30$.
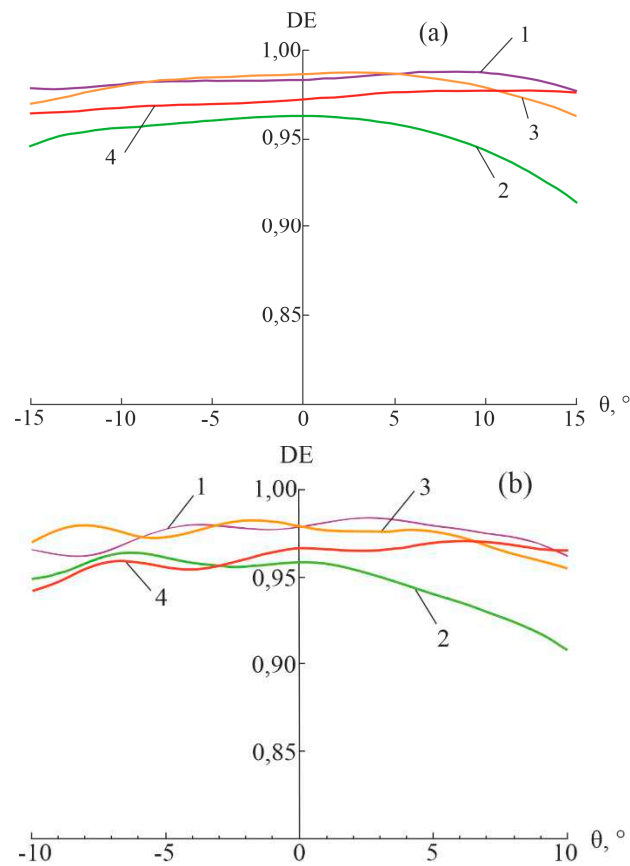
Figure 3. Dependences of the DE of E48R/EP7000 microstructure on the angle of incidence for multiple wavelengths: (a) $h_1 = 8.792$ μm, $h_2 = 6.268$ μm, and $P = 30$; and (b) $h_1 = 8.792$ μm, $h_2 = 6.246$ μm, and $P = 10$ ($1 - \lambda = 0.4$ μm, $2 - \lambda = 0.5$ μm, $3 - \lambda = 0.6$ μm, and $4 - \lambda = 0.7$ μm).

Considering that the oscillations are most pronounced at $P = 10$ and $\lambda = 0.7$ μm, the calculation is performed with these parameters for the case without antireflection coatings (Figure 4).
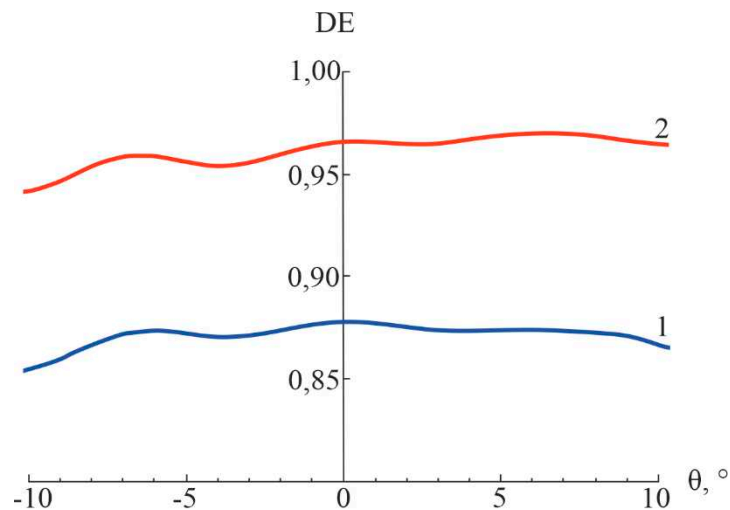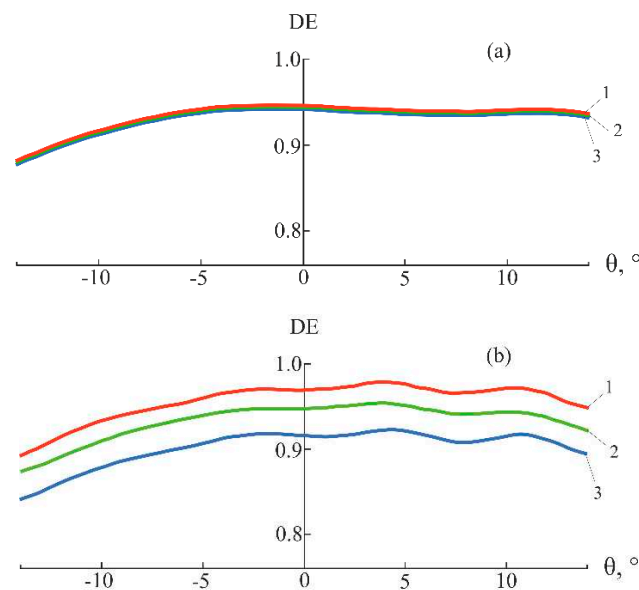
Figure 4. Dependences of the DE of E48R/EP7000 microstructure on the angle of incidence for $\lambda = 0.7$ μm and $P = 10$ (1 – without modeling of antireflection coatings and 2 – with modeling of antireflection coatings).

The calculation results presented in Figures 3 and 4 confirm that the oscillating nature of the dependence of DE on the angle of incidence is not associated with the Fresnel reflection of radiation from flat or relief working surfaces of the microstructure; moreover, these dependences are identically retained even after almost completely suppressing the reflections.

A novel in-depth analysis of the influence of the parameters L and N_m on the level of DE and oscillations is presented next. Moreover, E48R/EP7000 microstructure with the model antireflection coatings is used for analysis. In this case, the optical thicknesses of the plates in both layers are assumed equal, i.e., $L = n_1 \cdot l_{h1} = n_2 \cdot l_{h2} = k\lambda$. The analysis demonstrates that the optical thicknesses of the plates in the range of $0.08 \leq k \leq 0.32$ have almost no effect on the oscillations, but significantly affect the DE level. Furthermore, the number of modes ($50 \leq N_m \leq 600$) affects both the DE level and oscillations. These trends are clearly confirmed by the graphs in Figure 5 obtained at the central wavelength of the visible spectral range $\lambda = 0.55$ μm at $h_1 = 8.792$ μm, $h_2 = 6.246$ μm, and $P = 10$. At $N_m = 50$, the curves corresponding to all values of k merge, and the DE level is the lowest (Figure 5a). At $N_m = 200$, the oscillations are pronounced, and the DE level increases with decreasing k (Figure 5b). At $N_m = 400$, the oscillations decrease to an acceptable level, and the DE level, similar to that in Figure 5b, increases with decreasing k (Figure 5c). A further decrease in k leads to merging of the curves with a slight increase in the DE level (Figure 5d).

The calculation time increases with decreasing k and increases depending on N_m, usually according to a quadratic law. Accordingly, the maximum value of k and the minimum value of N_m can be used at which oscillations do not significantly affect the calculation results. In the case under consideration, $k \leq 0.12$ and $N_m = 300$ at $\lambda = 0.55$ μm (Figure 6a). Furthermore, at other wavelengths of the working spectral range, the oscillations can have a slightly larger amplitude, requiring a decrease in k to 0.08 and an increase in N_m to 400 for their almost complete suppression (Figure 6b).
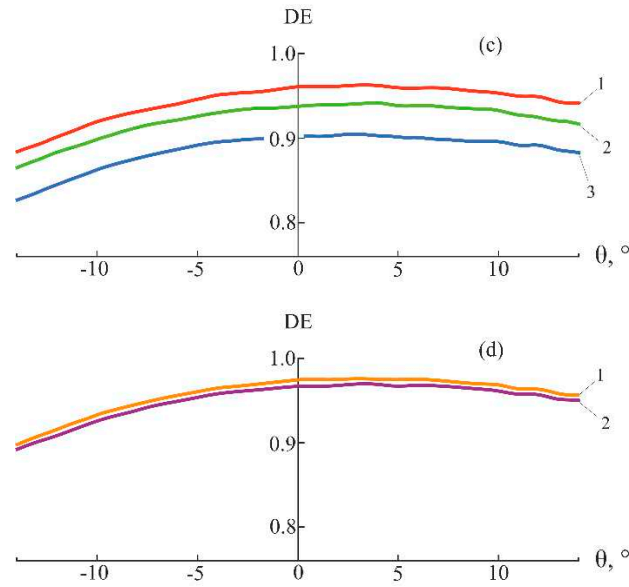
Figure 5. Dependences of the DE of E48R/EP7000 microstructure on the angle of incidence at a wavelength of $\lambda = 0.55$ μm at $P = 10$: (a) $N_m = 50$; (b) $N_m = 200$; and (c) $N_m = 400$ ($1 - k = 0.16$, $2 - k = 0.24$, and $3 - k = 0.32$). (d) $N_m = 400$ ($1 - k = 0.08$ and $2 - k = 0.12$).
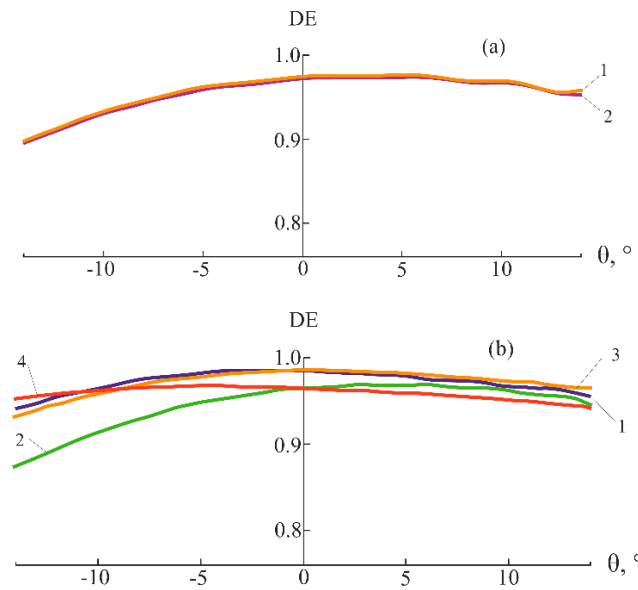

Figure 6. Dependences of the DE of E48R/EP7000 microstructure on the angle of incidence at $P = 10$: (a) $N_m = 300$ at a wavelength of $\lambda = 0.55$ μm ($1 - k = 0.08$ and $2 - k = 0.12$) and (b) $N_m = 400$ and $k = 0.08$ at four visible wavelengths ($1 - \lambda = 0.4$ μm, $2 - \lambda = 0.5$ μm, $3 - \lambda = 0.6$ μm, and $4 - \lambda = 0.7$ μm).

A double increase in the relative spatial period of the microstructure ($P = 20$) does not affect the recommended value of the k parameter ($k \leq 0.12$), but requires an increase in the recommended value of the N_m parameter ($N_m \geq 500$, see Figure 7).

Comparing the recommended N_m values obtained for this microstructure at $P = 10$ and $P = 20$, the following simple relation is valid:

$$N_m > P(h_1 + h_2)/\lambda, \tag{2}$$

where λ is the central wavelength of the working spectral range.

Note that, as pointed out in [7,20], an increase in the spatial period of the microstructure allows expanding the range of radiation incidence angles within which the DE does not fall below a given level.
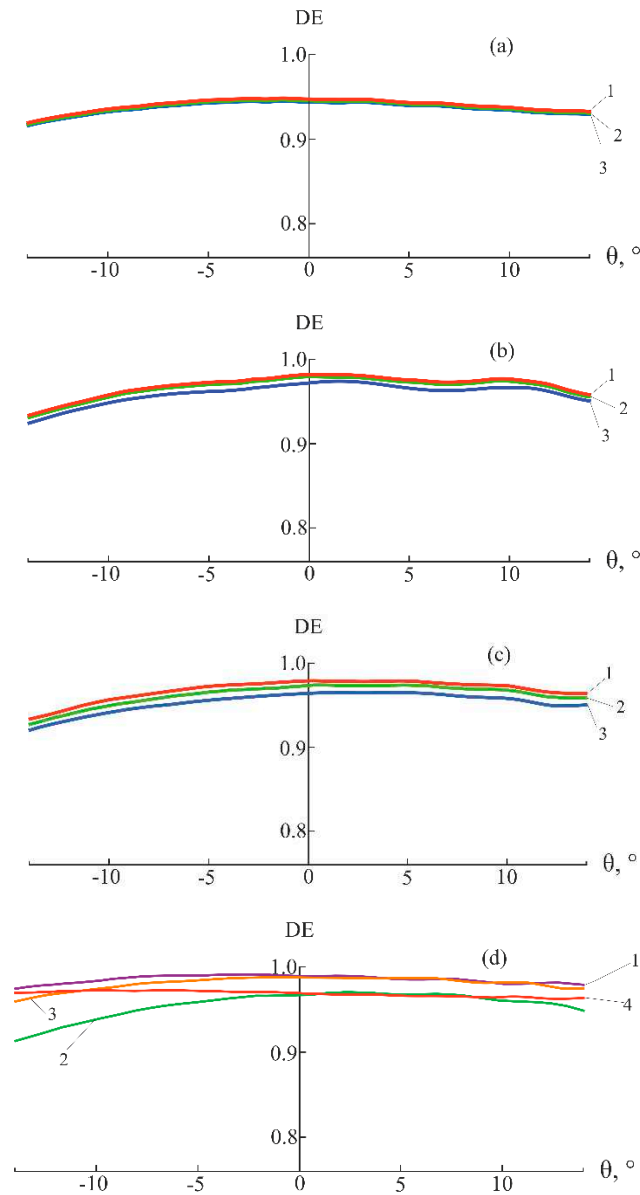

Figure 7. Dependences of the DE of E48R/EP7000 microstructure on the angle of incidence at $P = 20$: (a) $N_m = 50$ and $\lambda = 0.55$ μm; (b) $N_m = 400$ and $\lambda = 0.55$ μm; and (c) $N_m = 600$ and $\lambda = 0.55$ μm ($1 - k = 0.08$, $2 - k = 0.12$, and $3 - k = 0.16$). (d) $N_m = 600$ and $k = 0.08$ at four visible wavelengths ($1 - \lambda = 0.4$ μm, $2 - \lambda = 0.5$ μm, $3 - \lambda = 0.6$ μm, and $4 - \lambda = 0.7$ μm).

Similar calculations for two-layer microstructures with two internal sawtooth reliefs composed of pairs of optical plastics, namely, PMMA/POLYCARB, E48R/POLYSTYR, and E48R/ITO in PMMA [7] result in the same recommended k and N_m values. Moreover, this does not depend on whether PSUAC-DE or MC Grating Software is used for calculations.

3. Infrared spectral range

In this section, we investigate how optical thickness of the plates L and the number of modes Nm influence the relationship between the DE of microstructures and the angle of incidence of IR radiation. These microstructures belong to the DOEs of several refractive-diffractive objectives designed by the authors of this article. The objectives were designed to operate in the dual IR range,

including medium-wavelength IR (MWIR) (3.4-5.2 μm) and long-wavelength IR (LWIR) (7.5-11.4 μm) subranges.

The results of the study are demonstrated by the example of two microstructures SRF2/GERMANIUM (h_1 = 53.6 μm and h_2 = 8.71 μm) and PBF2/GASIR1 (h_1 = 87.36 μm and h_2 = 44.12 μm). Three materials of their layers (SRF2, PBF2, and GERMANIUM) are obtained from the INFRARED catalog of the ZEMAX program; moreover, GASIR1 is obtained from the UMICORE catalog [16]. The choice of these microstructures is not accidental. They both have a fairly high DE at $|\theta| \leq 14°$, whereas the refractive indices of the respective layers differ by more than 1.2 and 1.6 times (Table 1).

Table 1. Refractive indices of IR optical materials at the central wavelengths of the MWIR and LWIR subbands.

λ, μm	n_1		n_2	
	SRF2	PBF2	GERMANIUM	GASIR1
4.3	1.410538	1.714346	4.021764	2.509057
9.45	1.319191	1.646837	4.004906	2.496018

In the calculations, as in the visible range, the radiation is assumed to be incident on the microstructure from the air onto the side of the medium with the refractive index n_1, the angle of incidence θ is measured from the normal to the substrate, and the diffracted radiation remains in the medium with the refractive index n_2. In this case, the optical thicknesses of the plates in both layers are assumed equal, i.e., $L = n_1 \cdot l_{h1} = n_2 \cdot l_{h2} = k\lambda$.

Figure 8 shows the dependence curves of the DE for the SRF2/GERMANIUM microstructure with regards to the angle of incidence, obtained using PSUAC-DE program at P = 10.
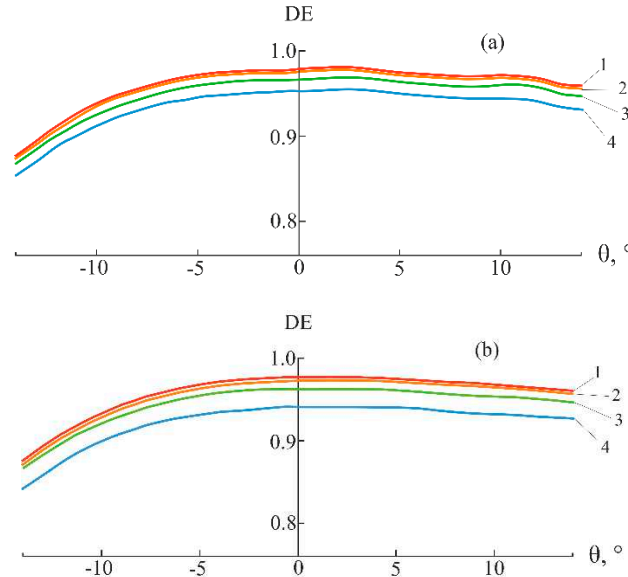

Figure 8. Dependences of the DE of SRF2/GERMANIUM microstructure on the angle of incidence for a wavelength of λ = 4.3 μm and P = 10: (a) N_m = 200 and (b) N_m = 400 (1 – k = 0.05, 2 – k = 0.075, 3 – k = 0.1, and 4 – k = 0.15).

At N_m = 200, the oscillations are insignificant, whereas at N_m = 400, they disappear completely. In this case, a k value of less than 0.05 does not make sense. This is true for all dual-IR wavelengths (Figure 9).

A two-fold increase in the relative spatial period of the microstructure in this case does not affect the recommended value of the parameter k, but requires an increase in the number of modes to reduce the oscillation amplitude to an acceptable level (Figures 10 and 11).
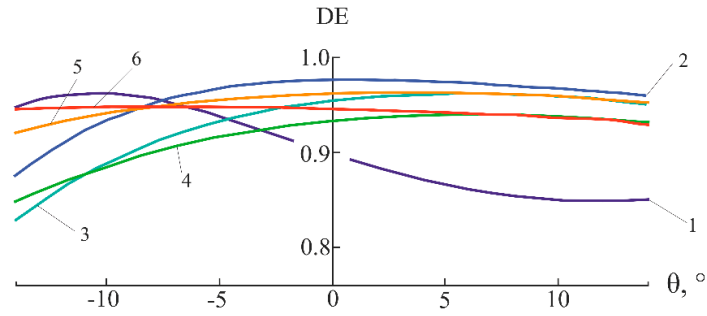
Figure 9. SRF2/GERMANIUM DE versus angle of incidence at $P = 10$, $N_m = 400$, and $k = 0.05$ for six dual-IR wavelengths: $1 - \lambda = 3.4$ μm, $2 - \lambda = 4.3$ μm, $3 - \lambda = 5.2$ μm, $4 - \lambda = 7.5$ μm, $5 - \lambda = 9.45$ μm, and $6 - \lambda = 11.4$ μm.
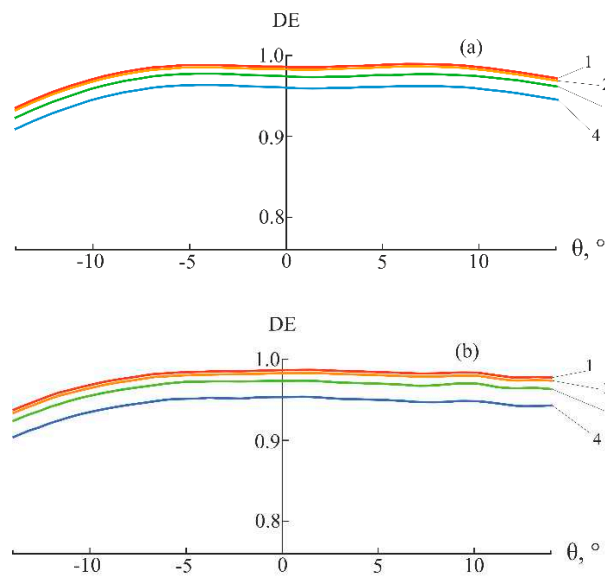

Figure 10. Dependences of the DE of SRF2/GERMANIUM microstructure on the angle of incidence for a wavelength of $\lambda = 4.3$ μm and $P = 20$: (a) $N_m = 200$ and (b) $N_m = 400$ ($1 - k = 0.05$, $2 - k = 0.075$, $3 - k = 0.1$, and $4 - k = 0.15$).
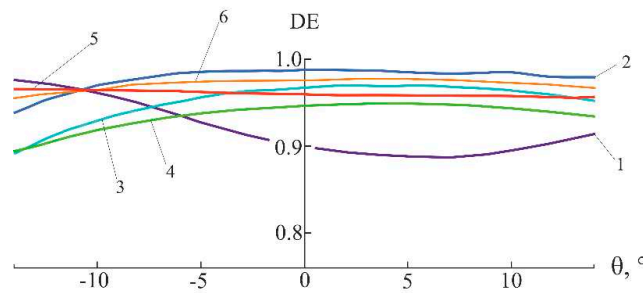

Figure 11. SRF2/GERMANIUM DE versus angle of incidence at $P = 20$, $N_m = 400$, and $k = 0.05$ for six dual-IR wavelengths: $1 - \lambda = 3.4$ μm, $2 - \lambda = 4.3$ μm, $3 - \lambda = 5.2$ μm, $4 - \lambda = 7.5$ μm, $5 - \lambda = 9.45$ μm, and $6 - \lambda = 11.4$ μm.

By comparing the k values used in the visible and IR ranges as well as the refractive indices of E48R/EP7000 and SRF2/GERMANIUM microstructures, the following empirical formula is proposed for the relationship between the corresponding k values:

$$k_{IR} \approx k_{Vis} n_2^{(Vis)} \big/ n_2^{(IR)}, \tag{3}$$

where k_{IR} and k_{Vis} are the k parameters of the second layer of the microstructure at the central wavelengths of the MWIR and visible ranges, respectively. Similarly, $n_2^{(IR)}$ are $n_2^{(Vis)}$ are the corresponding refractive indices.

An analysis of the influence of the k and N_m parameters on the level and oscillations of the DE of PBF2/GASIR1 microstructure is conducted at the values of k calculated using Equation (3). The results for $P = 10$ case are presented in Figure 12.
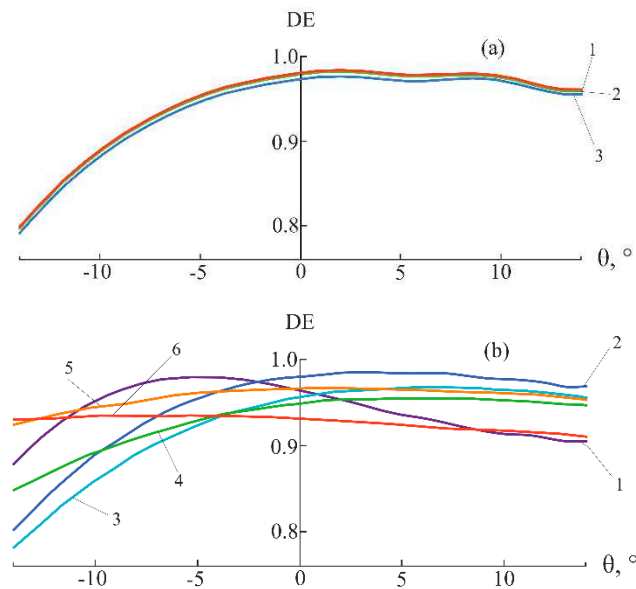

Figure 12. Dependences of the DE of PBF2/GASIR1 microstructure on the angle of incidence at $P = 10$: (a) $N_m = 200$ for a wavelength of $\lambda = 4.3$ μm ($1 - k = 0.105$, $2 - k = 0.158$, and $3 - k = 0.21$) and (b) $N_m = 400$ and $k = 0.105$ for six wavelengths of dual IR ($1 - \lambda = 3.4$ μm, $2 - \lambda = 4.3$ μm, $3 - \lambda = 5.2$ μm, $4 - \lambda = 7.5$ μm, $5 - \lambda = 9.45$ μm, and $6 - \lambda = 11.4$ μm).

An increase in the relative spatial period of the microstructure to $P = 20$ does not affect the recommended value of the parameter k in the case of this microstructure; however, a two-fold increase in the number of modes is required, which reduces the oscillation amplitude to an acceptable level.

Note that in the IR and visible ranges, an increase in the spatial period of the microstructure allows expanding the range of radiation incidence angles within which the DE does not fall below a given level.

Summarizing the results presented in Sections 2 and 3, the value provided by Equation (2) should be considered as the recommended number of modes for all microstructures in both the visible and IR ranges. As for the parameter k, based on formula (3), it should be taken as its recommended value k ≤ 0.264/n2, where n2 is the larger of the two refractive indices of the microstructure layers at the central wavelength of the visible or MWIR ranges.

Obviously, an increase in the relative spatial period, which allows expanding the range of angles of incidence of radiation incident on the microstructure, inevitably increases the computational complexity of the RCWA calculation of the DE.

4. Discussion

In several previous studies, the results of using a rigorous diffraction theory based on the solution of Maxwell equations for calculating the DE of multilayer sawtooth microstructures have been presented [6–9,11,17–23].

However, in these studies devoted to the use of the FDTD and RCWA methods for calculating the DE of single-layer binary and sawtooth microstructures, as well as for calculating the DE of two-layer one- or two-relief sawtooth microstructures, the problem of minimizing the computational complexity of these methods has not been considered. At best, individual recommendations aimed

at reducing computational process time have been cited without evidence. Furthermore, the computational complexity of electromagnetic methods often exceeds that of scalar methods. This problem stimulated the search for a new effective method for arranging and calculating two-relief microstructures within the framework of the scalar theory of diffraction, considering the real depths of sawtooth reliefs. To this end, EAM has been proposed [9,10]. The advantage of EAM is that it allows truly selecting the optimal pairs of optical materials for sawtooth two-layer two-relief microstructures intended for operation in both the visible and IR ranges [8]. However, a reliable estimate of the optimal relief depths and DE levels of such microstructures within the given ranges of radiation incidence angles in multiple cases can only be obtained through optimization within the framework of a rigorous diffraction theory. The practical possibility of such an optimization is primarily determined by the computational complexity of the DE calculations. This study successfully investigates and substantiates the conditions for minimizing the computational complexity of the RCWA method.

5. Conclusions

The DOE of imaging optical systems in both the visible and IR ranges must have a high DE within the working spectral range and within a given range of angles of incidence of radiation incident on the microstructure. These requirements are satisfied, in particular, by the elements with a sawtooth two-layer two-relief microstructure. In this case, a reliable and optimal pair of optical materials for such a microstructure can be selected within the framework of the scalar theory of diffraction. However, truly optimal relief depths and a reliable assessment of the DE level of the microstructure within a given range of radiation incidence angles can be obtained, in most cases, only as a result of electromagnetic optimization, particularly using the RCWA method. The accuracy of this method is determined by the optical thicknesses of the flat lattice slabs $L = n_1 \cdot l_{h1} = n_2 \cdot l_{h2} = k\lambda$ that make up both the microreliefs and the number of modes N_m, i.e., the harmonics of the Fourier series. The computational complexity of the calculations also depends on these parameters.

The recommendations proposed and substantiated in this study on selecting the number of modes and optical thickness of the plates (Equations (2) and (3)) allow minimizing the computational complexity of the RCWA calculation of the DE of a sawtooth two-layer two-relief microstructure while maintaining the specified reliability of the calculation results.

Moreover, the computational complexity can be controlled through the relationship $N_m = C\Lambda/\lambda$, i.e., by allowing one or another level of oscillation of the DE curves depend on the angle of incidence. By setting $C \leq 1$, the complexity of multiple DE calculations can be reduced in the optimization process. Moreover, by setting $C > 1$, the computational complexity can be increased to certify the accuracy of the solution obtained as a result of implemented optimization.

References

1. Greisukh, G.I.; Bobrov, S.T.; Stepanov, S.A. *Optics of diffractive and gradient-index elements and systems*; Bellingham: SPIE Press, 1997; 414 p.
2. Wood, A.; Babington, J.; *Diffractive Lens Design: Theory, design, methodologies and applications (Emerging Technologies in Optics and Photonics)*; Iop Publishing Ltd, 2023; 300 p.

3. Arieli, Y.; Ozeri, S.; Eisenberg, N. Design of a diffractive optical element for wide spectral bandwidth. *Opt. Lett.* 1998, 23(11), 823–824.

4. Lukin, A.V. Holographic optical elements. *Journal of Optical Technology.* 2007, 74(1), 65–70. https://doi.org/10.1364/JOT.74.000065

5. Zhao, Y.H.; Fan, C.J.; Ying, C.F.; Liu, S.H. The investigation of triple-layer diffraction optical element with wide field of view and high diffraction efficiency. *Opt. Com.* 2013, 295, 104–107. http://dx.doi.org/10.1016/j.optcom.2013.01.009

6. Greisukh, G.I.; Yezhov Y.G.; Antonov, A.I.; Danilov, V.A.; Usievich, B.A. Potential opportunities of sawtooth diffraction microstructure with two layers and single relief. *Journal of Optics.* 2020, 22(8), 085604. https://doi.org/10.1088/2040-8986/ab90ce

7. Greisukh, G.I.; Danilov, V.A.; Ezhov, E.G.; Kazin, S.V.; Usievich, B.A. Highly Efficient Double-Layer Diffraction Microstructures Based on New Plastics and Molded Glasses. *Photonics.* **2021**, 8, 327. https://doi.org/10.3390/photonics8080327

8. Greisukh, G.I.; Ezhov, E.G.; Antonov, A.I.; Danilov, V.A.; Usievich, B.A. Comparative analysis estimates for two-relief microstructures diffraction efficiency in the visible and dual infrared ranges in the framework of scalar and rigorous diffraction theories. *Journal of Optical Technology.* 2023, **90**(3), xx-xx. **(in print)**

9. Yang, H.; Xue, C.; Li, C.; Wang, J; Zhang, R. Diffraction efficiency sensitivity to oblique incident angle for multilayer diffractive optical elements. *Appl. Opt.* 2016. 55(25), 7126–7133. https://doi.org/10.1364/AO.55.007126

10. Yang, C.; Yang, H.; Li, C.; Xue, C. Optimization and analysis of infrared multilayer diffractive optical elements with finite feature sizes. *Appl. Opt.* 2019, 58, 2589–2595. https://doi.org/10.1364/AO.58.002589

11. Moharam, M.G.; Pommet, D.A.; Grann, E.B.; Gaylord, T.K. Stable implementation of the rigorous coupled-wave analysis for surface-relief gratings: enhanced transmittance matrix approach. *JOSA.* 1995, 12(5), 1077–1086. https://doi.org/10.1364/JOSAA.12.001077

12. Antonov, A.I.; Greisukh, G.I.; Kazin, S.V. Certificate of state registration of the computer program «PSUAC-DE» № 2022681578 (Russian Federation), 2022.

13. Lyndin, N.M. Modal and C Methods Grating Design Available online: http://www.mcgrating.com (accessed on 12 April 2023).

14. Zemax Source. Available online: http://www.zemax.com/pages/opticstudio (accessed on 12 April 2023).

15. Mitsubishi Gas Chemical. Available online: http://www.mgc.co.jp/eng/products/kc/iupizeta_ep.html (accessed on 12 April 2023).

16. UMICORE Electro-Optic Materials Source. Available online: https://eom.umicore.com/en/infrared-solutions/infrared-optics/intrsoducing-gasir (accessed on 12 April 2023).

17. Hakko, M.; Kiire, T.; Barada, D.; Yatagai, T.; Hayasaki, Y. Shape estimation of diffractive optical elements using high-dynamic range scatterometry. *Applied Optics.* 2015, 54(13), 4255–4261. https://doi.org/10.1364/AO.54.004255

18. Di, F.; Yingbai, Y.; Guofan, J.; Qiaofeng, T.; Liu, H. Rigorous electromagnetic design of finite-aperture diffractive optical elements by use of an iterative optimization algorithm. JOSA A. 2003, 20(9), 1739–1746. https://doi.org/10.1364/JOSAA.20.001739

19. Lee, Y.J.; Kim, Y.H.; Park, C.M.; Yang, J.K. Analysis of optical propagation characteristics of the ultra-long period grating using RCWA. *Applied Optics.* 2023, 62(9), 2376–2385. https://doi.org/10.1364/AO.483184

20. Greisukh, G.I.; Levin, I.A.; Ezhov, E.G. Design of Ultra-High-Aperture Dual-Range Athermal Infrared Objectives. *Photonics.* **2022**, 9, 742. https://doi.org/10.3390/photonics9100742

21. Bo Zhang, Qingfeng Cui, Mingxu Piao. Effect of substrate material selection on polychromatic integral diffraction efficiency for multilayer diffractive optics in oblique incident situation. *Opt. Commun.* 2018, 415, 156–163. https://doi.org/10.1016/j.optcom.2018.01.043

22. Francés, J.; Bleda, S.; and al. Accuracy analysis of simplified and rigorous numerical method sapplied to binary nanopatterning gratings in non-paraxial domain. *Physics Letters A.* 2013. Vol. 377. P. 2245–2250. https://doi.org/10.1016/j.physleta.2013.05.059

23. Qing Xu; Xinrong Chen; Chaoming Li; Yangling Guo; Xu Chen; Yong Xu. Design of 2-layer transmission grating with high efficiency, large bandwidth and great dispersion. *Proc. SPIE.* 11551, Holography, Diffractive Optics, and Applications X, 115511D, 2020. https://doi.org/10.1117/12.2573369